Open Heavy-Flavour Photoproduction at NLO

Gustav Kramer

II. Institut für Theoretische Physik, Universität Hamburg, Luruper Chaussee 149, D-22761 Hamburg, Germany

Abstract. We review the construction of non-pertubative fragmentation functions for $D^{*\pm}$ mesons, both at leading and at next-to-leading order in two different subtraction schemes in the so-called massless approach. The fragmentation functions are determined by fitting to OPAL and ALEPH data on inclusive $D^{*\pm}$ production in e^+e^- annihilation. It is shown, how recent data on inclusive $D^{*\pm}$ photoproduction in ep collisions at HERA are reproduced with two sets of fragmentation functions differing in the subtraction schemes. The influence of different assumptions on the charm distribution of the photon is pointed out.

1 Introduction

The production of heavy-flavoured hadrons (with charm or bottom) in the colliding beam experiments with HERA provides new opportunities to study the dynamics of perturbative QCD and to obtain information on the proton and photon structure. Heavy-flavour production at HERA is dominated by photoproduction events, where the electron (or positron) is scattered by a small angle producing photons of almost zero virtuality. In this case the electron scattering is equivalent to the scattering of on-shell photons carrying a fraction of the electron energy distributed according to the Weizsäcker-Williams spectrum [1]. The dynamics of charm and bottom photoproduction can be probed at HERA in a large kinematical region, the available center-of-mass energy being one order of magnitude larger than in fixed target experiments. As is well known, photoproduction at HERA is described with two mechanisms, direct photoproduction, where the photon interacts directly with the quarks coming out of the proton, and via resolved photon interactions, where the photon fluctuates into parton constituents (quarks or gluons), which undergo hard scattering with the partons from the proton. Two types of approaches have been pursued in the calculation of photoproduction cross sections for heavy-flavour production in next-to-leading order (NLO). In the massive approach [2] one assumes that light quarks and gluons are the only active flavours within the ingoing proton and photon. In this approach the heavy quark mass $m_Q \gg \Lambda_{QCD}$ acts as a cutoff for initial and final state singularities and sets the scale for the perturbative calculation. The cross section factorizes into a partonic hard-scattering cross section multiplied by light-quark and gluon densities. In this so-called massive quark scheme, the number of active flavours in the initial state is $n_f = 3$, if charm and bottom are treated as massive, and, for example, $n_f = 4$, if only the bottom quark

is considered massive. For the prediction of the total charm or bottom photoproduction cross section this is the only possibility. The massive approach is also the correct approach for the production of heavy flavoured hadrons with transverse momenta $p_T^2 \simeq m_Q^2$. If $p_T^2 \gg m_Q^2$, mass terms in the hard scattering cross sections are suppressed by powers of m_Q/p_T, but potentially large terms $\propto \ln(p_T^2/m_Q^2)$ arise from the collinear branching of gluons or photons into heavy quark-antiquark pairs or from the collinear emission of a gluon by a heavy quark at large transverse momentum. For $p_T \gg m_Q$ these terms spoil the convergence of the pertubation series and must be summed by absorbing the collinear $\ln(p_T^2/m_Q^2)$ singular terms into heavy-quark parton density functions (PDF's) of the proton or photon, respectively, or into fragmentation functions (FF's) of the heavy quark into the heavy hadron. An alternative way to the absorption of the large logarithm into parton densities and fragmentation functions is to treat the heavy quark Q as massless from the start and to absorb the collinear singularities into PDF's and FF's in the same way as it is done for the lighter u, d and s quarks using the standard $\overline{MS}$ subtraction scheme. This allows for the consistent usage of the standard NLO parton densities with $n_f = 4$ ($n_f = 5$) flavours for the proton or photon which have been constructed in this scheme. This way of calculating heavy-flavour production has been denoted the massless scheme [3]. The mass of the heavy quark appears only in the starting scale of the c or b quark parton distribution functions of the proton and the photon and the fragmentation functions of the heavy quarks, c or b, into heavy flavoured hadrons. In the case of hadrons containing bottom quarks only the total photoproduction cross section has been measured so far [4], so that the massless approach has not become relevant yet.

For the production of charmed mesons, both H1 [5] and ZEUS [6,7] have presented experimental results for $D^{*\pm}$ photoproduction. This channel is favoured because of its clear experimental signal coming from the $D^* \to D\pi$ decay with subsequent decay of the D into $K\pi$ and $K\pi\pi\pi$ channels. The data cover the p_T range up to $p_T \simeq 10.5\ GeV$ [5] and $p_T \simeq 12\ GeV$ [6,7], so that at least for the data in the high p_T range the massless scheme should be applicable. In the medium p_T range it is conceivable that the massive (fixed-order) and the massless (resummed) approach are equally reliable, and only in the low-p_T range $p_T \simeq m_c$ the massive scheme is preferred.

In the massless scheme it is also easy to incorporate information on the fragmentation of c quarks into D^* mesons from other processes, as for example $e^+ + e^- \to D^* + X$, into photoproduction of D^*'s at HERA, since, according to the general factorization theorems, this information is universal and can be used for the prediction of any inclusive D^* production process in terms of universal FF's for $c \to D^*$. This information on the $c \to D^*$ FF's comes from high-energy e^+e^- data from LEP, where several data sets for $e^+e^- \to D^*X$, older [8,9] and newer [10,11] ones, exist, which have been used to determine the FF's of D^*'s employing two different subtraction schemes.

In this report I shall review the influence of different descriptions of the fragmentation process inside the resummed approach, valid for $p_T \gg m_c$, on the

predictions of inclusive D^* production in ep collisions at HERA. I shall give a comparison with ZEUS data only in cases relevant for the comparison of these different approaches. A more complete confrontation of the recent H1 [5] and ZEUS [6,7] data with the different theoretical approaches, massive and massless, has been presented elsewhere at this workshop [12] and in the H1 [5] and ZEUS [6,7] papers.

In the next section I shall give a short account of the NLO formalism for massless partons. In sect. 3 the calculation of the fragmentation functions for D^* mesons based on two different schemes is reviewed. Sect. 4 contains a discussion of their consequences for the inclusive photoproduction of D^*'s at HERA. In sect. 5 I finish with some conclusions and an outlook to possible work in the future.

2 NLO Formalism for Massless Partons

The calculation of the NLO inclusive cross section for the production of a hadron h with transverse momentum p_T and rapidity y in the resolved mode starts from the formula

$$\begin{aligned}\frac{d^3\sigma}{dy\,d^2p_T} = \frac{1}{\pi}\sum_{a,b,c}\int dx_\gamma dx_p \frac{dx_h}{x_h^2}\, F_a^\gamma(x_\gamma, M_\gamma^2) F_b^p(x_p, M_p^2)\, D_c^h(x_h, M_h^2) \\ \left[\frac{d\sigma_{ab\to c}^0}{dt}(s,t,u,\mu^2)\,\delta\left(1+\frac{t+u}{s}\right)\right. \\ \left. + \frac{\alpha_s(\mu^2)}{2\pi} K_{ab\to c}(s,t,u,\mu^2,M_\gamma^2,M_p^2,M_h^2)\,\theta\left(1+\frac{t+u}{s}\right)\right], \quad (1)\end{aligned}$$

where $s=(p_a+p_b)^2$, $t=(p_a-p_c)^2$ and $u=(p_b-p_c)^2$. The NLO corrections [13] $K_{ab\to c}$ comprise 16 channels and their $t\to u$ crossed counterparts. $d\sigma_{ab\to c}^0/dt$ stands for the LO hard-scattering cross sections for the transition $ab\to cX$, where $X=d$ is a single parton in LO. F_a^γ and F_b^p are the PDF's of the photon and proton, respectively, which must be calculated at scales M_γ and M_p with the help of the NLO evolution equations derived for the $\overline{MS}$ subtraction scheme. Similarly, D_c^h denots the FF for $c\to h$ (in our case $h=D^{*\pm}$) evolved up to the scale M_h, also in the $\overline{MS}$ subtraction scheme. We emphasize that the summation over parton labes a, b and c includes also the charm quark. This means, that the charm quark is also present in the initial state inside the proton and particularly inside the photon.

The formula for $\gamma+p\to h+X$ via direct photoproduction can be deduced from (1) by the replacements

$$\begin{aligned} F_a^\gamma(x_\gamma, M_\gamma^2) &\to \delta(1-x_\gamma), \\ d\sigma_{ab\to c}^0 &\to d\sigma_{\gamma b\to c}^0, \\ K_{ab\to c} &\to K_{\gamma b\to c}. \end{aligned} \quad (2)$$

At LO, only the photon-gluon fusion process $\gamma g\to q\bar{q}$ and the Compton process $\gamma q\to gq$ contribute. NLO corrections [14] $K_{\gamma b\to c}$ include eight channels. It is

well known that NLO corrections lead to a reduction of the dependence on the renormalization scale μ and the factorization scales M_γ, M_p and M_h This way, they reduce the theoretical uncertainty and lead in certain regions of phase space to sizable shifts in the cross section due to additional parton emissions in the final state. It should also be mentioned, that in NLO the definition of direct and resolved cross section looses its meaning. At higher orders only their sum is uniquely defined and can be compared to experimental data.

The derivation of these formulas is done in dimensional regularization, which is needed to extract the ultraviolet, infrared and collinear divergencies. Since the charm quark is considered massless as all the other quark flavours, divergencies originating from the cg collinear singularities are encountered, which are absorbed into the bare PDF's and FF of the photon, proton and D^* meson. At this step finite terms in the NLO matrix elements $K_{ab\to c}$ remain, which are fixed by selecting the $\overline{MS}$ subtraction scheme. In the massive scheme these collinear singularities are cut off by the finite quark mass m_c and no subtraction is necessary. In addition, there are no bare PDF's or FF's in this scheme, which could absorb the subtraction terms.

3 Fragmentation Functions for D^*

Several different procedures to describe the fragmentation of c quarks into D^*'s have been developed. They differ whether and how information for the production of massive quarks in e^+e^- annihilation is included in the transition $c \to D^*$. They are described by introducing the function $D_a^C(x,\mu^2,m_c^2)$ for the transition of a massless parton a (including the massless charm quark c) to a massive c quark (denoted C). These functions have been derived by Mele and Nason [15] by matching the cross section $d\sigma(e^+e^- \to C+X)/dx$, where all powers of m_c^2/s have been neglected, in the massive scheme ($m_c \neq 0$) to the cross section $d\sigma(e^+e^- \to a\bar{a}+X)$ in the massless scheme ($m_c = 0$ from the beginning). The result is

$$\frac{d\sigma_{e^+e^-\to C+X}}{dx}(x,s,m_c^2) = \sum_a \int_x^1 \frac{dz}{z} D_a^C\left(\frac{x}{z},\mu^2,m_c^2\right) \frac{d\sigma_{e^+e^-\to a+X}}{dz}(z,s,\mu^2) \quad (3)$$

where

$$D_a^C(x,\mu^2,m_c^2) = \delta_{aC}\delta(1-x) - \frac{\alpha_s(\mu^2)}{2\pi} d_{a\to C}(x,\mu^2,m_c^2) \quad (4)$$

$$d_{a\to C}(x,\mu^2,m_c^2) = -P_{q\to q}^{(0,T)}(x)\ln\frac{\mu^2}{m_c^2} + \frac{4}{3}\left\{-2\delta(1-x) + 2\left(\frac{1}{1-x}\right)_+ + 4\left[\frac{\ln(1-x)}{1-x}\right]_+ - (1+x)[1+2\ln(1-x)]\right\} \quad (5)$$

$$d_{g\to C}(x,\mu^2,m_c^2) = -P_{g\to q}^{(0,T)}(x)\ln\frac{\mu^2}{m_c^2} \quad (6)$$

$$d_{q,\bar{q},\bar{c}\to C}(x,\mu^2,m_c^2) = 0 \quad (7)$$

This formula can be interpreted in many ways. Of course, when $D_a^C(x,\mu^2,m_c^2) = \delta_{aC}\delta(1-x)$, the left hand side of (3) is just the cross section for $e^+e^- \to c\bar{c}+X$ with massless c quarks. If, on the other hand, the remaining terms in D_a^C are moved to the hard scattering factor $d\sigma(e^+e^- \to a+X)/dx$, we recover the formula for the production of massive c quarks at NLO up to the neglected terms proportional to m_c. μ is the factorization scale for the massless cross section, which is usually chosen as $\mu = \sqrt{s}$, where s is the squared center-of-mass energy. When $\mu = \sqrt{s} \simeq 2m_c$ the formula (3) with (4) and (5) can be used directly as it stands. When $\mu = \sqrt{s} \gg m_c$ large logarithms appear which must be summed. To preserve the structure contained in $d_{a\to C}(x,\mu^2,m_c^2)$ for finite m_c the function (4) is assumed to determine the FF for $a \to C$ at the starting scale $\mu_0 \simeq m_c$, and one calculates the FF at larger scales μ via the usual Altarelli- Parisi equations [16]. It follws from (5) that the evolution is given by the well known massless evolution kernel $P_{q\to q}^{(0,T)}(x)$. In this way these so-called perturbative FF's are fully determined concerning the μ dependence and also the initial conditions. Only the starting scale μ_0 has to be chosen appropriately. This approach with pertubative FF's was first applied to the calculation of cross sections for the production of b quarks in hadron-hadron collisions [17] and later to the production of c quarks in γp [18] and $\gamma\gamma$ collisions [19] based on the massless scheme described in the previous section. Later it became clear that the pertubative FF as just described is not sufficient to predict cross sections for the production of heavy flavoured hadrons, like D^* mesons, and $D_a^C(x,\mu^2,m_c^2)$ must be convoluted with a non-pertubative FF $D_C^{D^*}(x,\mu_0^2)$ which accounts for the transition $C \to D^*$ [18]. This FF can not be calculated in pertubation theory. It is asumed to be universal, so that it can be fixed by comparing with one set of experimental data and then used to predict other D^* production cross sections. It has been obtained from inclusive $e^+ + e^- \to D^* + X$ cross sections measured at DORIS and LEP [18]. It is clear that with this procedure the total fragmentation $a \to D^*$, starting from the massless c quark a, is a convolution of the pertubative FF with the non-pertubative FF.

Instead of introducing the concept of a pertubative component for the FF one can incorporate the difference between the massless and massive cross section for $e^+ + e^- \to C + X$ in a different way, namely, by combining the terms in D_a^C proportional to $d_{a\to C}$ with the hard scattering cross section $d\sigma(e^+e^- \to a+X)/dz$ in the sense of changing the final-state factorization scheme. This amounts to substituting in the hard-scattering cross section

$$\alpha_s(\mu^2)\,P_{a\to c}^{(0,T)}(x)\ln\frac{s}{\mu^2} \to \alpha_s(\mu^2)\,P_{a\to c}^{(0,T)}(x)\ln\frac{s}{\mu^2} - \alpha_s(\mu_0^2)d_{a\to C}(x,\mu_0^2,m_c^2) \quad (8)$$

One should note that the coupling in front of $d_{a\to C}$ is evaluated at the input scale μ_0. This shift leaves the cross section for massive charm production for scales $\mu \simeq \mu_0 \simeq m_c$ unchanged, when $D_a^C(x,\mu^2,m_c^2) = \delta_{aC}\delta_{aC}(1-x)$ is retained. In [20] it was shown that this way of incorporating the differnce of the massless and massive hard-scattering cross section is consistent with the cross section for $e^+ + e^- \to C + X$ including all terms up to $O(\alpha_s^2)$ in the leading logarithmic approximation. It is clear that when this change of final-state fac-

torization scheme is performed for calculating the $e^+e^- \to D^*X$ cross section, in order to construct the FF's for $a \to D^*$ from experimental data, it must be intoduced also in all other hard-scattering cross sections for predicting inclusive D^* production. This change of the final-state factorization has been used for studying the influence of various approximations in the fragmenation of D^* mesons in [21] and somewhat later for predicting photoproduction cross sections with fragmentation information coming from LEP experiments in [22].

The method of combining pertubative and non-pertubative FF's in the analysis of D^* production at DORIS and LEP for the calculation of NLO inclusive D^* photoproduction cross sections has been applied in [18] and reviewed by Cacciari at the 1997 Workshop [23]. As already said, it turned out that the fragmentation of charm or bottom quarks into D^* mesons cannot be calculated from first principles in pertubation theory. In fact, in order to realistically desribe the formation of the D^* meson, a non-pertubative component, which is not known theoretically, is always needed. Hence, it is appropriate to give up the pertubative component of the FF input altogether and to describe the $c \to D^*$ and $b \to D^*$ transitions entirely by non-pertubative FF's, as it also done for the fragmentation of u, d and s quarks into light mesons. This is the basis of our recent work [24], which has been compared with the new ZEUS and H1 experimental results in [6,7] and [5] (see also [12]). It should be clear that the parameters of the non-pertubative FF's differ, depending on whether a pertubative component of the FF is introduced (via the initial conditions respectively via a change of the subtraction scheme) or not.

The construction of the non-pertubative FF's for $c \to D^*$ by fitting large-s data on $e^+ + e^- \to D^* + X$ is complicated since in hadronic Z decays charmed mesons are expected to be produced either directly through the hadronization of charm quarks in the process $Z \to c\bar{c}$ or via weak decays of B hadrons produced in $Z \to b\bar{b}$ with approximately equal rate. Charmed mesons from $Z \to c\bar{c}$ allow us to measure the c-quark FF. The main task of the experimental analysis was to disentangle these two main sources of $D^{*\pm}$ production at the Z boson resonance. In our first analysis, in which the $d_{a\to C}$ subtraction scheme was used, we made use of the LEP data from ALEPH [8] and OPAL [9].

The starting scales for the D^* FF's of the gluon and the u, d, s and c quarks and antiquarks was set to $\mu_0 = 2m_c$ with $m_c = 1.5\ GeV$, whereas for bottom it was set to $\mu_0 = 2m_b$ with $m_b = 5\ GeV$. The FF's of the gluon and the first three quark flavours are assumed to be zero at the starting scale. For the parametrization of charm- and bottom quark FF's at their respective starting scales two different forms were employed, the so-called standard (S) and mixed (M) sets [22]. Here we review only the results with the mixed set. The results with the standard set are very similar and lead to almost identical predictions for the photoproduction of D^*'s. In the mixed set the FF of the bottom quark is assumed to be of the form

$$D_b^{D^{*\pm}}(x, \mu_0^2) = N x^\alpha (1-x)^\beta \tag{9}$$

which contains three parameters and is best suited for FF's which peak at smaller x. The charm-quark FF at the initial scale is equal to the Peterson distribution

[25]

$$D_c^{D^{*\pm}}(x,\mu_0^2) = N\frac{x(1-x)^2}{[(1-x)^2+\epsilon x]^2} \tag{10}$$

which is particularly suitable to describe FF's that peak at large x. It depends only on two free parameters, N and ϵ. Both ALEPH [8] and OPAL [9] extracted the total $D^{*\pm}$ momentum distribution as well as the individual contributions due to $Z \to c\bar{c}$ and $Z \to b\bar{b}$. In the performed LO (NLO) analysis the one-loop (two-loop) formula for α_s with $\Lambda^{(5)}_{\overline{MS}} = 108\ MeV$ $(227\ MeV)$ was used. The obtained values of N, α, β and ϵ resulting from the combined LO (NLO) fits to the ALEPH and OPAL data are given in [22]. The ϵ parameter in the LO (NLO) fit is $\epsilon = 0.0856$ (0.0204). In the NLO fit ϵ is very much reduced since part of the fragmentation is described by the pertubative component. In Fig. 1 the fits are compared to the OPAL [9] data. For the fits to the ALEPH data see [22]. Both, the LO and NLO results are shown. Except for very small x, the LO and NLO curves are very similar. At small x large differences occur, indicating that in this region the pertubative treatment ceases to be valid. Also, in this region, the massless approximation is not valid anymore. In any case, due to the finite D^* mass, the D^* can only be produced for $x > x_{min} = 2m(D^*)/M_Z = 0.046$. This is the region, where the NLO results turn negative. Therefore the results are meaningful only for $x > x_{cut} = 0.1$. For the fitting actually only the x bins in the interval $[0.1, 0.9]$ were used. The quality of the fit measured in terms of average χ^2 for all selected data points is quite good. Details are found in [22]. Also the branching fractions of the two transitions $c \to D^*$ and $b \to D^*$ which are calculated from the FF's over x in the interval $x_{cut} < x < 1$ came out in agreement with the measured values: $B_c = 0.259$ and $B_b = 0.252$ [9] with errors of 25%. The corresponding theoretical values are 0.231 (0.221) and 0.215 (0.219) for the LO (NLO) fit. These numbers show that we have the correct normalization. Another quantity of interest is the mean momentum fraction $< x >_Q (\mu)$ where $Q = c, b$. This depends on the scale, where it is evaluated. For $\mu = M_Z$ we have $< x >_c = 0.490$ (0.556) for the LO (NLO) FF, which has to be compared to $< x >_c = 0.495^{+0.010}_{-0.011} \pm 0.007$ [8] and $< x >_c = 0.515^{+0.008}_{-0.005} \pm 0.010$ [9].

Looking at the curves in Fig. 1 we notice that the NLO fits lead to negative cross sections in the vicinity of $x = 1$. This is directly conneted with the subtraction of the pertuabative $d_{a\to C}$ functions. To remove this unphysical behaviour one must resum the pertubative contributions for $x \to 1$ originating from the finite mass cross section. Also due to this extra complication the description in terms of pure non-pertubative FF's is preferred. Negative cross sections at $x \leq 1$ occur also in all the other formulations with pertubative pieces in the FF's [18,26]. With the same ALEPH [8] and OPAL [9] data we performed fits also in the truly massless scheme discarding the pertubative contributions in form of the $d_{a\to C}$ functions. Here the fit could be done in the interval $[0.1, 1]$ in contrast to the fit with the $d_{a\to C}$ functions, which was limited to $[0.1, 0.9]$. The main difference in the NLO fit was a change of the Peterson parameter to

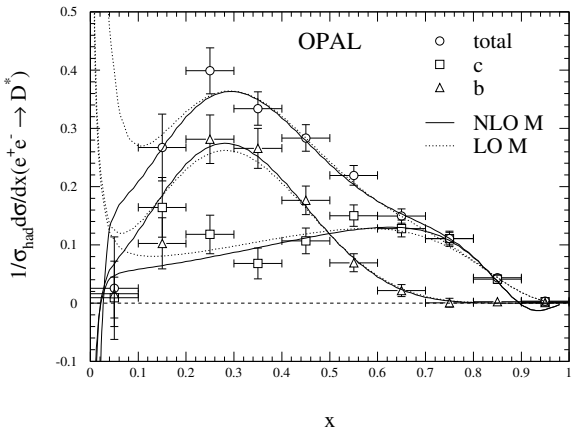

Fig. 1. Comparison of the OPAL data [10] on $e^+ + e^- \to D^{*\pm} + X$ with the LO M (dashed) and NLO M (solid) calculations. The three sets of curves and data correspond to the $Z \to c\bar{c}$ and $Z \to b\bar{b}$ samples as well as their combination.

$\epsilon = 0.116$. The fit was equally good, the χ^2 changed only from 0.96 to 1.01. Of course, also the fragmentation parameters for $b \to D^*$ fragmentation changed somewhat, but much less than the parameters for the c fragmentation.

In 1997 more precise data for $e^+ + e^- \to D^{*\pm} + X$ from ALEPH [10] and OPAL [11] became available. These new samples are compatible with the respective older samples, but not with each other. Both ALEPH [10] and OPAL [11] presented momentum distributions for their full $Z \to D^{*\pm} + X$ sample and for the $Z \to b\bar{b}$ subsample, but not separately for $Z \to c\bar{c}$ as in the previous measurements. We used the new data to perform only fits without the $d_{a\to C}$ subtraction. The fit parameters for the two data sets in LO and NLO and for the two flavours c and b are displayed in Tab. I of [24]. The obtained parameters for ALEPH and OPAL come out different indicating that the two data sets do not overlap inside their errors. Both sets have much larger ϵ parameters in NLO compared to the earlier fits with the massive subtraction. In Fig. 2 the OPAL [11] data are compared with the sets LO O and NLO O (O stands for OPAL). The comparison of the corresponding LO and NLO fits to the ALEPH data can be found in Fig. 1b of [24]. Except at very small x, the LO and NLO results are again very similar. There are large differences between the LO and NLO parameters obtained from the same data. The value $\epsilon = 0.0851$ of set LO O is very similar to $\epsilon = 0.0856$ of the set obtained from the older data [8,9]. Compared to the NLO fit with the $d_{a\to C}$ subtraction shown in Fig. 1, the new NLO fit in Fig. 2 stays positive also for $x \geq 0.9$, coincides there with the LO result, and nicely describes the data.

As with the fits to the older data, we studied also the branching fractions and the mean momentum fractions for the two sets and compared them with the available experimental information. Both quantities turned out to be in

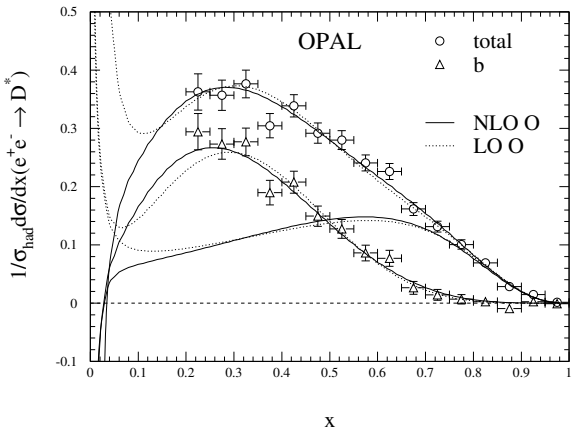

Fig. 2. Comparison of the OPAL data [12] on $e^+e^- \to D^{*\pm} + X$ with the LO O (dashed) and NLO O (solid) calculations. The three sets of curves correspond to the $Z \to c\bar{c},\ Z \to b\bar{b}$ and full samples.

reasonable agreement with the data, details are found in [24]. We tested also, whether the FF's constructed from LEP data lead to a consistent description of $e^+e^- \to D^*X$-data at lower energies. This presents a direct test of the underlying scaling violations of fragmentation via the time-like Altarelli-Parisi equations. The comparison with data from ARGUS [27] at $\sqrt{s} = 10.49\ GeV$, from HRS [28] at $\sqrt{s} = 29\ GeV$ and from TASSO [29] at $\sqrt{s} = 34.2\ GeV$ calculated with the LO and NLO OPAL and ALEPH sets can be seen in in Fig. 2a,b of [24] together with the OPAL and ALEPH data, respectively. The agreement with all the data is quite good. These comparisons assure us that the $D^{*\pm}$ FF's, although constructed from data at $\sqrt{s} = M_Z$, lead to a valid description of $D^{*\pm}$ fragmentation at lower scales.

Based on the universality of fragmentation we have made predictions for inclusive $D^{*\pm}$ photoproduction at HERA. The results for the FF's based on the older LEP data and empoying the massive charm subtraction scheme are found in [22] as well as the comparison with the ZEUS data [30] published in 1997. The more recent H1 [5] and ZEUS [6,7] have been compared only with the more recent predictions based on FF's obtained with the recent ALEPH and OPAL results and without the massive subtraction. Such comparisons have been shown also at the workshop in Coldewey's contribution [12]. In [24] we compared with preliminary ZEUS data from their 1996 analysis [31]. In the next section I shall present some of these results with particular emphasis on how the two fragmentation schemes, with and without the massive subtraction, influence the predictions. In addition I shall discuss the contribution of the resolved cross section.

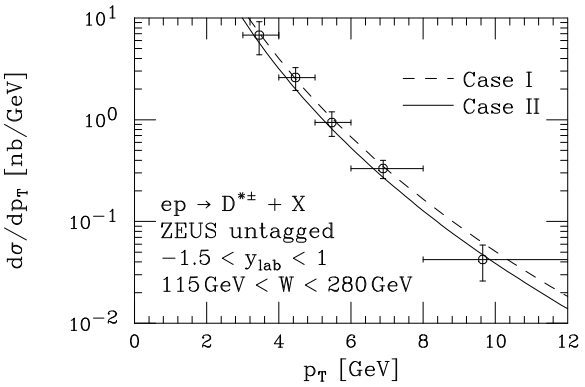

Fig. 3. Comparison of the ZEUS data on $e+p \to D^{*\pm}+X$ with the NLO calculations according to cases I (dashed) and II (solid).

4 $D^{*\pm}$ Production in Low-Q^2 ep Collisions

It is clear that the cross section for inclusive $D^{*\pm}$ production in low-Q^2 ep collisions at HERA depends on input from different sources. First, it depends on the way the FF for the $D^{*\pm}$ is constructed. In [21] several versions of approximating the D^* fragmentation have been investigated. For example, in [21] the ϵ parameter in the Peterson fragmentation formula was varied by ± 0.02. This changed the cross section by $\pm 15\%$ with the branching fraction fixed to its experimental value. This is not a very large change. Since in our more recent work [22,24] the D^* FF was fixed by LEP data this dependence on the FF is largely eliminated. The final prediction, though, may still depend on the scheme used to construct the fragmentation in NLO. i.e. with or without the massive subtraction terms. When we fitted to the LEP data, we also had to take into account $D^{*\pm}$ production by bottom-quark fragmentation. In ep collisions, however, the bottom quark does not contribute to $D^{*\pm}$ production below the threshold at $m_T = \sqrt{p_T^2 + m_c^2} = m_b$. In contrast to e^+e^-- annihilation the bottom quark does not contribute significantly even above threshold. In [22] we found that the relative contribution due to the b-quark FF's is below 5% and decreases with increasing p_T.

Another issue is the problem of the scheme dependence in the construction of the FF's. Above we presented the results for $D^{*\pm}$ FF's obtained from fitting the same LEP data, but with the different schemes, one with and one without the massive subtraction $d_{a\to C}$. As we have seen, these two schemes lead to completely different non-pertubative components in NLO, expressed by two completely different ϵ parameters, $\epsilon = 0.0204$ and $\epsilon = 0.116$, respectively. In Fig. 3 I show the predictions for the $D^{*\pm}$ photoproduction cross section with the two schemes. The dashed curve (case I) is with $d_{a\to C}$ subtraction and the full curve (case II) without. In Fig. 3 the p_T distributions $d\sigma/dp_T$ is compared to the older ZEUS [30] data. We observe, that the two predictions differ approximately by

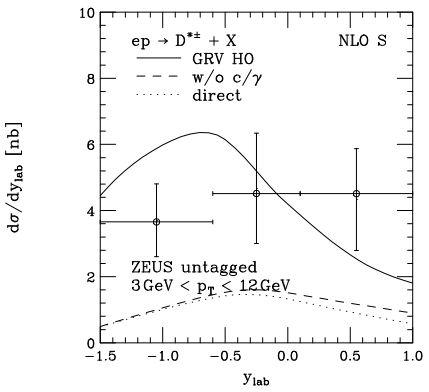

Fig. 4. Sensitivity to the charm content of the photon.

25%. We think that this difference is characteristically the error caused by using two different fragmentation approaches. We note that the cross section with the massive subtraction lies higher than without the subtraction, which is based on the pure $\overline{MS}$ factorization. This is in contrast to the predictions of Cacciari et al. [18], where the $d_{a\to C}$ functions are taken into account via the initial conditions of the FF's. Although these two approaches are equivalent up to $O(\alpha_s^2)$ in the logarithmic terms, they differ in nonlogarithmic terms in the same order. We assume that this difference in the treatment of the $d_{a\to C}$ terms is the explanation for the smaller D^* photoproduction cross sections in [18].

The largest uncertainty in the calculation of the $D^{*\pm}$ photoproduction cross section is related to the charm content of the resolved photon. The most sensitive distributions to study this dependence are the differential rapidity distributions for fixed p_T. To illustrate the sensitivity to the charm PDF of the photon, the NLO analysis (here with the NLO S fragmentation function and with the FF in the massive subtraction scheme from [22]) with this PDF switched off is shown in Fig. 4 and compared to the full calculation. We observe that 73% to 100% (50% to 89%) of the resolved (full) cross section is induced by the charm content of the photon, which is most important in the backward direction. In Fig. 4 the cross section is plotted as a function of y_{lab}, integrated over $3 < p_T < 12\,GeV$. We emphasize, the lower p_T limit may be somewhat too small to justify the massless scheme. A larger p_T limit should be suited better. However, here the influence of the resolved component diminishes somewhat. The three experimental points are from the first ZEUS measurements [30].

It is well known, that the pure massive scheme [2] contains a contribution from the charm component in the photon. This is hidden in the NLO corrections to the direct cross section. As long as all m_c^2/p_T^2 terms are negligible this contribution, in a first approximation, should be equivalent in the massless scheme to the LO resolved component. Therefore it is of interest to see the influence of the NLO corrections to the resolved component since this contribution is certainly absent in the massive scheme. This is shown in Fig. 5, where the NLO

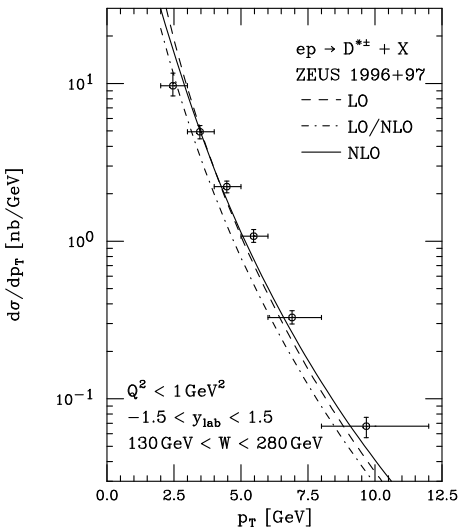

Fig. 5. Comparison of the ZEUS data on $e + p \to D^{*\pm} + X$ with the LO O (dashed) and NLO O (solid) calculations. The dot-dashed curve emerges from the solid one by switching off the NLO terms in the partonic cross sections of the resolved processes.

O calculation of $d\sigma/dp_T$ is compared to the case, where the NLO terms in the partonic cross sections are switched off. For $p_T \geq 5\ GeV$ we observe an increase of up to 50% due to the NLO corrections. This is almost the difference between the results of the massive scheme and the massless scheme, as can be seen in Fig. 2 of [6]. In Fig. 5 the most recent ZEUS data [6] are compared to the full NLO massless calculation of [24]. The experimental data lie somewhat above the predicted results, in particular for the larger p_T values, where the agreement actually should be better. The difference amounts to approximately 30% (not considering the experimental errors) for $p_T > 5\ GeV$. In Fig. 5 we plotted also the LO O prediction. It is very similar to the NLO O result showing good pertubative stability. We emphasize that the LO curves are obtained with LO PDF's, FF's and the one-loop formula for α_s.

We have seen above that the charm component of the resolved photon makes an important contribution to the $D^{*\pm}$ photoproduction cross section. All the results shown so far are obtained with the parametrization of GRV in LO or NLO [32]. It is interesting to see the results for other photon PDF's. Such comparisons are shown in Fig. 6, where the differential rapidity distributions are plotted after integration over four different p_T ranges $p_{T,min} < p_T < 12\ GeV$ with $p_{T,min} = 2, 3, 4$ and $6\ GeV$. Besides GRV the photon PDF's of Gordon and Storrow (denoted GS92) [33] and two others from Aurenche et al. for massless charm quarks [34] denoted AFG and for massive charm quarks [35] denoted ACFGP(m_c) are employed. We observe a significant variation of the cross sections, especially also in the backward direction. The difference is particularly

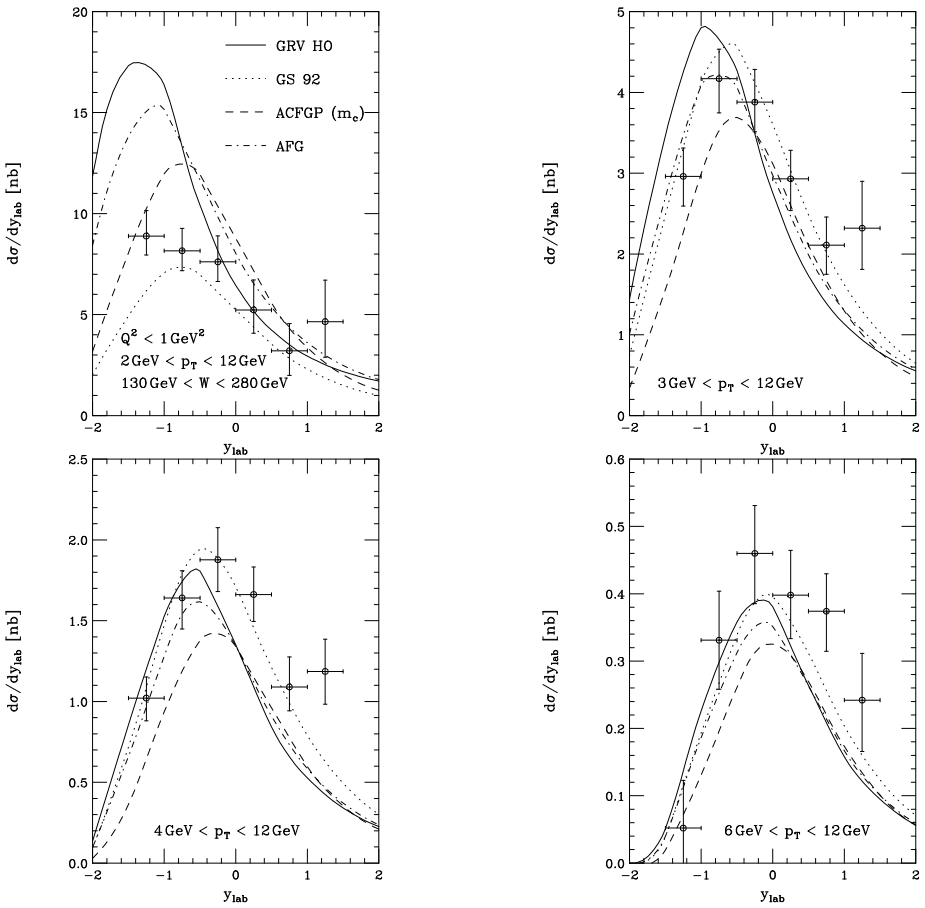

Fig. 6. Comparison of the ZEUS data on $e+p \to D^{*\pm}+X$ with the NLO O calculation for different photon PDF's.

marked for the curves with $p_{T,min} = 2\ GeV$. For $p_{T,min} = 6\ GeV$ the differences are much less. In this figure the various predictions are also compared to the recent ZEUS data [6]. Of course, for $p_{T,min} = 2\ GeV$ we would not expect that the massless scheme yields reliable predictions, although the GS92 curve comes close to the data. All other PDF's give too large cross sections in this case. Also for the other $p_{T,min} = 3, 4$ and $6\ GeV$ the GS92 prediction agrees reasonably well with the data points, but also GRV and AFG agree for the two largest $p_{T,min}$'s. The GS92 prediction is also better in the forward direction where the deviation between the data and the prediction is largest.

Very recently the ZEUS collaboration also presented data in a smaller total center-of-mass energy region W, $80 < W < 120\ GeV$ [7] compared to the high W region $130 < W < 280\ GeV$ already published [6]. The p_T and y_{lab} intervals of these data are $2 < p_T < 8\ GeV$ and $-1 < y_{lab} < 1.5$. The predicted $d\sigma/dp_T$

distribution based on our fragmentation approach without the massive subtraction and $\epsilon = 0.116$ is in good agreement with the data. The cross section as a function of y_{lab} integrated over the region $3.25 < p_T < 8\ GeV$ agrees best with the newer Gordon-Storrow photon PDF [36] (see [7]), although some access in the forward region is still evident if compared to the prediction.

5 Conclusions

The study of inclusive $D^{*\pm}$ production in e^+e^- and ep collisions allows for a meaningful test of the QCD-improved parton model. Inside the massless approach, where the charm-quark mass is neglected, we discussed two different subtraction schemes for the fragmentation functions in NLO. Both can be used to fit $D^{*\pm}$ production at LEP and lead to comparable photoproduction cross sections at HERA. It is emphazised that the fit results for the input parameter ϵ of the Peterson et al. parametrization is highly scheme dependent at NLO and must not be naively compared disregarding the theoretical framework which it refers to.

A large part of the $D^{*\pm}$ photoproduction cross section originates from the resolved process, eventually allowing to determine the charm distribution function of the photon more accurately. The reasonable agreement between the NLO masslesss theory and recent $D^{*\pm}$ photoproduction data from ZEUS is quite encouraging. This is also true for the $\gamma\gamma \to D^{*\pm}X$ process, for which new data were shown at this workshop [37]. It is pointed out, that the theoretical cross section is particularly enhanced by the NLO corrections to the resolved component, a contibution, which is absent in any pure massive calculation. It is understood, that the massless-quark approximation is only appropriate for $D^{*\pm}$ production at large enough p_T, say $p_T > 4\ GeV$. So it should not be expected to yield meaningful predictions for the photoproduction at small-p_T $D^{*\pm}$ mesons at HERA. The next step in theory would be to retain the finite charm-quark mass and to subtract in the NLO corections to the direct process the colllinear logarithmic mass divergences in such a way that the $\overline{MS}$ subtracted massless theory is aproached in the limit $m_c \to 0$. This formulation should be applicable at small and large p_T.

Acknowledgements

This work was supported by Bundesministerium für Forschung und Technologie, Bonn, Germany, under Contract 05 7 HH 92P (0), and by the EU Fourth Framework Program *Training and Mobility of Researchers* through Network *Quantum Chromodynamics and Deep Structure of Elementary Particles* under Contract FMRX–CT98–0194 (DG12 MIHT). I would like to thank J. Binnewies, B. A. Kniehl and M. Spira for their collaboration and B. A. Kniehl for help with the manuscript.

References

1. C. F. v. Weizsäcker, Z. Phys. 88 (1934) 612; E. J. Williams, Phys. Rev. 45 (1934) 729
2. S. Frixione, P. Nason and G. Ridolfi, Nucl. Phys. B454 (1995) 3 and the earlier references given there
3. B. A. Kniehl, M. Krämer, G. Kramer and M. Spira, Phys. Lett. B356 (1995) 539
4. D. Pitzl in these Proceedings
5. C. Adloff et al., H1 Collaboration, Nucl. Phys. B545 (1999) 21
6. J. Breitweg et al., ZEUS Collaboration, Eur. Phys. J. C6 (1999) 67
7. Y. Eisenberg, On behalf of the ZEUS Collaboration, Talk given at DIS99, 19-23 April 1999, Zeuthen, Germany, hep-ex/9905008
8. D. Buskulic et al., ALEPH Collaboration, Z. Phys. C62 (1994) 1
9. R. Akers et al., OPAL Collaboration, Z. Phys. C67 (1995) 27
10. ALEPH Collaboration, Contributed Paper No. 623 to the International Europhysics Conference on High Energy Physics, Jerusalem, Israel, 1997 and CERN/EP 99-094, July 8, 1999
11. K. Ackerstaff et al., OPAL Collaboration, Eur. Phys. J. C1 (1998) 439
12. C. Coldewey in these Proceedings
13. F. Aversa, P. Chiapetta, M. Greco and J.-Ph. Guillet, Nucl. Phys. B327 (1989) 105
14. P. Aurenche, R. Baier, A. Douiri, M. Fontannaz and D. Schiff, Nucl. Phys. B286 (1987) 553; L. E. Gordon, Phys. Rev. D50 (1994) 6753
15. B. Mele and P. Nason, Nucl. Phys. B361 (1991) 626
16. G. Altarelli and G. Parisi, Nucl. Phys. B126 (1977) 298
17. M. Cacciari and M. Greco, Nucl. Phys. B421 (1994) 530
18. M. Cacciari and M. Greco, Z. Phys. C69 (1996) 459; Phys. Rev. D55 (1997) 7134
19. M. Cacciari, M. Greco, B. A. Kniehl, M. Krämer, G. Kramer and M. Spira, Nucl. Phys. B466 (1996) 173
20. P. Nason and C. Oleari, Phys. Lett. B418 (1998) 199
21. B. A. Kniehl, G. Kramer and M. Spira, Z. Phys. C76 (1997) 689
22. J. Binnewies, B. A. Kniehl and G. Kramer, Z. Phys. C76 (1997) 677
23. M. Cacciari, Proceedings of the Ringberg Workshop, New Trends in HERA Physics edited by B A Kniehl, G Kramer, A Wagner, World Scientific, Singapore-New Jersey-London-Hong Kong
24. J. Binnewies, B. A. Kniehl and G. Kramer, Phys. Rev. D58 (1998) 014014
25. C. Peterson, D. Schlatter, I. Schmitt and P. M. Zerwas, Phys. Rev. D27 (1983) 105
26. P. Nason and O. Oleari, Phys. Lett. B447 (1999) 327; hep-ph/9903541, submitted to Nucl. Phys. B
27. H. Albrecht et al., ARGUS Collaboration, Z. Phys. C52 (1991) 353
28. P. Barninger et al., HRS Collaboration, Phys. Lett. B206 (1988) 551
29. W. Braunschweig et al., TASSO Collaboration, Z. Phys. C44 (1989) 365
30. J. Breitweg et al. ZEUS Collaboration, Phys. Lett. B401 (1997) 192
31. ZEUS Collaboration, Contributed Paper No 653 to the International Europhysics Conference on High Enery Physics, Jerusalem, Israel, 1997
32. M. Glück, E. Reya and A. Vogt, Phys. Rev. D46 (1992) 1973
33. L. E. Gordon and J. K. Storrow, Z. Phys. C56 (1992) 307
34. P. Aurenche, J.-Ph. Guillet and M. Fontannaz, Z. Phys. C64 (1994) 621
35. P. Aurenche, P. Chiapetta, M. Fontannaz, J.-Ph. Guillet and E. Pilon, Z. Phys. C56 (1992) 589
36. L. E. Gordon and J. K. Storrow, Nucl. Phys. B489 (1997) 405
37. R. Nisius in these Proceedings